Sensors and Materials, Vol. 35, No. 10 (2023) 4511–4525
MYU Tokyo

S & M 3411

Antenna Sensor Array Design for Structural Strain and Crack Monitoring

Chen-xu Xu,[1] Yuan-hao Wang,[2] Yun-fei Li,[1] Hao Cai,[2*] and Guo-dong Han[2]

[1]Special Equipment Safety Supervision Inspection Institute of Jiangsu Province, Nanjing 210036, China
[2]School of Transportation and Logistics Engineering, Wuhan University of Technology, Wuhan 430063, China

(Received July 21, 2023; accepted September 26, 2023)

Keywords: antenna sensor array, frequency division multiplexing, structural strain, crack length, structural health monitoring

In this study, we designed an antenna sensor array for integrated strain and crack monitoring to understand the monitoring parameters of individual sensors and address the challenge of detection over a large area. First, the design method for the antenna sensor array was investigated on the basis of the strain and crack monitoring principles of antenna sensors. Frequency division multiplexing was implemented in the design of the antenna sensor array to differentiate the resonant frequency information of each array element. Then, the patch layout, patch size, and feed network were designed to form the model of the antenna sensor array, and the strain and crack monitoring capability of the cracked antenna sensor array was analyzed through simulation. Finally, the feasibility of using an antenna sensor array for the integrated strain and crack monitoring of structures was experimentally verified. The theoretical analysis, simulation, and experimental results reveal that the designed antenna sensor array can monitor the integrated strain and crack information of the structure, and the crack monitoring sensitivity of the crack monitoring patch is approximately 13.1 MHz/mm. The strain monitoring sensitivities in the horizontal, vertical, and 45° directions are 1.0783, 1.9466, and 0.7127 kHz/με, respectively.

1. Introduction

Under long-term alternating loads, cracks that form in the vulnerable parts of metal structures will continue to expand, which destroys the integrity of the metal structure. Additionally, the stress concentration in the cracked parts also inevitably reduces the load-bearing capacity of the metal structure and leads to accidents such as structural fractures. Therefore, to ensure the safety and stability of metal structures and prevent accidents, it is important to monitor structure damage. This enables overall structural health supervision and regular maintenance.(1)

Standard structural health sensors (including but not limited to eddy current sensors,(2) ultrasonic detection sensors,(3) optical fiber sensors,(4) and metal foil strain gauges(5)) can be used in structural health monitoring to some extent. However, there are many

*Corresponding author: e-mail: 320529@whut.edu.cn
https://doi.org/10.18494/SAM4598

ISSN 0914-4935

shortcomings, including (1) single sensor function, (2) independent data transmission and sensor functions, and (3) complex wiring. Microstrip antenna sensors are capable of detecting structural cracks and strain, and transmitting data as sensor units. Passive wireless technology allows for easy installation and conformation with complex structures when using microstrip antenna sensors. Furthermore, if there are structures that necessitate widespread area surveillance, the sensors can be readily integrated into an array to increase the monitoring scope. [6,7] Therefore, the use of antenna sensors has gained significant interest among numerous researchers.

To date, many domestic and overseas studies on the parameters of microstrip antenna sensors used for monitoring have been conducted, and crack parameters such as the crack length,[8] width,[9] depth,[10] and direction in metal structures and the structural strain magnitude and direction have been successfully monitored.[11–14] Owing to the small size of microstrip antenna sensors and their restricted monitoring range, which is limited to metal structures covered by patches, research on antenna sensor arrays has become essential in engineering practice to achieve a more extensive range of structural health monitoring. In 2012, Xu and Huang designed a binary antenna sensor array to monitor crack extension.[15] The differentiation of resonant frequency signals was achieved by the frequency and space division multiplexing methods. For the experimental structure, the sensor array achieved crack monitoring over a large area, and the resonant frequency of the sensor array elements decreased parabolically with the crack extension. In 2013, Yi *et al.* designed a three-patch sensor array to measure the strain without a feed line connected between the three patches; instead, the sensor array was interrogated by wireless monitoring.[16] The experimental results revealed that the electromagnetic interference between the patches affected the sensitivity of strain measurement, but the resonant frequency of each sensor and the strain were still linearly related to each other, which better facilitated the monitoring of structural strain. In 2014, Daliri *et al.* investigated the effect of the circular microstrip patch antenna (CMPA) design on the sensor quality factor and maximum practical wireless reading range.[17] The experimental results showed that the mass factor of CMPA has a significant effect on the wireless reading range. In 2018, Chakaravarthi *et al.* proposed a reusable passive sensor for wireless strain measurement on metal specimens.[18] The experimental results showed that the sensor response can be used to infinitely measure the stress and strain of the specimen with low error. In 2019, Herbko and Lopato developed a sensor consisting of two patches of different sizes.[19] The results of the tests showed that the sensor can be used both to measure the stress and determine its direction. Liu *et al.* designed an antenna sensor line array for detecting cracks in welds.[20] This array was arranged in a single line between the sensor array elements of the same size, and the delay line principle of the array differentiated the signals of the array elements. The experimental results revealed that the sensor array could accurately identify the location of weld cracks according to the change in resonant frequency, and the sensitivity of the sensor array for crack monitoring was approximately 5 MHz/mm. In 2022, Herbko *et al.* designed and investigated various fractal patches applied to microstrip strain sensing.[21] The experimental results showed that such fractals

can significantly reduce the patch size compared with rectangular patches. Chen *et al.* designed a novel chipless radio frequency identification (RFID) strain sensing tag to characterize the magnitude and direction of metal surface strain.[22] The experimental results show that the resonant frequency of the rectangular patch antenna unit with a chip decreases with increasing transverse compression or increasing longitudinal tensile strain, and the resonant frequency of the rectangular patch antenna unit with a chip increases with increasing longitudinal compression or increasing transverse tensile strain.

Existing research on antenna sensor arrays still faces challenges related to single-parameter measurement. This limitation restricts the current capabilities of antenna sensor arrays because they can only identify local structural crack or strain information. However, it is not easy to make an overall assessment of the health status of the local structure through the information transmitted by the sensor array. The increase in the number of excitation ports increases the wiring difficulty and the cost of monitoring equipment. Therefore, there is an urgent need to design an antenna sensor array structure that can be used in integrated strain and crack monitoring to improve the design and application of antenna sensor arrays and solve the multiparameter monitoring problem of antenna sensor arrays.

To meet the demand for monitoring the strain and cracks of metal structures, we designed an antenna sensor array using the frequency division multiplexing method in this study. Moreover, an antenna sensor array model was constructed, and the resonant frequency variation law of each unit of the antenna array under dynamic crack expansion and stress change was analyzed. The parameter monitoring capability of the proposed antenna sensor array was verified through testing.

2. Principles of Crack and Strain Monitoring Using Antenna Sensor Array

Figure 1(a) shows that the primary antenna sensor consists mainly of a metal radiation patch, a dielectric substrate, and a metal grounding layer. An electromagnetic resonant cavity, which is formed between the radiating patch and the metal grounding layer, radiates electromagnetic signals outwards. There are two main modes of operation: the TM10 mode where the current flows lengthwise and the TM01 mode where the current flows widthwise. The radiation

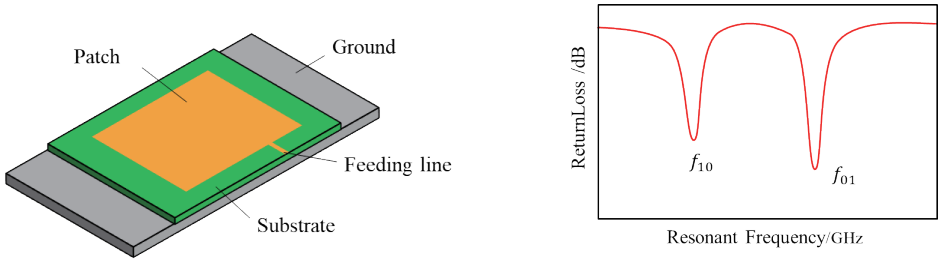

Fig. 1. (Color online) (a) Basic structure of microstrip antenna sensor and (b) typical S_{11} curve.

characteristics can be represented by the S_{11} curve shown in Fig. 1(b), whose trough corresponds to the resonant frequency of the sensor's fundamental operating frequency, which is also a critical object for monitoring the antenna sensor parameters.

The resonant frequency of the antenna sensor can be calculated using Eq. (1), where f_r is the resonant frequency of the sensor, ε_{eff} is the effective dielectric constant, ε_r is the relative dielectric constant of the substrate, c is the speed of light in vacuum, L is the current length (in the ideal strain-free case with the geometric length and width of the patch, when the radiation patch length L and width W are taken, corresponding to the resonant frequencies f_{10} and f_{01}), h is the thickness of the substrate, and ΔL is the line electrical length increment due to edge effects.[23]

$$f_r = \frac{c}{2\sqrt{\varepsilon_{eff}\left(L + 2\Delta L\right)}} \tag{1}$$

$$\varepsilon_{eff} = \frac{\varepsilon_r + 1}{2} + \frac{\varepsilon_r - 1}{2}\left(1 + 10\frac{h}{W}\right) \tag{2}$$

$$\Delta L = 0.412h\frac{\left(\varepsilon_e + 0.3\right)\left(W/h + 0.264\right)}{\left(\varepsilon_e - 0.258\right)\left(W/h + 0.813\right)} \tag{3}$$

The antenna sensor array is shown in Fig. 2. Patch 1 is the crack monitoring module. Its center is fed in such a way that when a crack develops and expands underneath it, Patch 1 can transmit information about the crack through resonant frequency translation. This allows for the effective monitoring of the crack expansion. Patches 2 and 3 are omnidirectional strain monitoring modules. Patch 2 is eccentrically fed to monitor the vertical and horizontal strains, and Patch 3 is centrally fed to monitor strains in the 45° direction. The flower-like structure formed by combining these two patches allows for measuring the strain values on the surface in

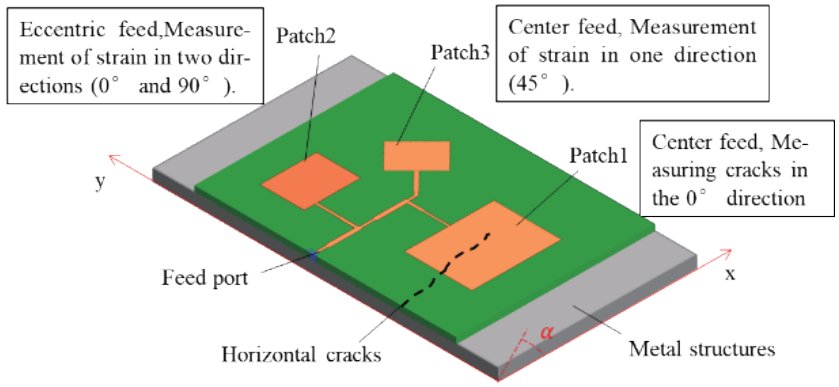

Fig. 2. (Color online) Schematic diagram of the antenna sensor array.

all three directions to determine the primary strain magnitude and direction of the flat structure.

As shown in Fig. 3, when cracks appear on the structure's surface, the resonant cavity surface current will bypass the current, leading to a change in the resonant frequency of Patch 1. According to Eq. (1), the resonant frequency of the responding patch antenna decreases as the crack length increases. Since there are no surface cracks beneath Patches 2 and 3, their resonant frequencies remain unchanged.

As shown in Fig. 4, when the tested metal structure is loaded, each patch will deform through stress transfer; the dashed line represents the shape of the deformed patch. From Eq. (1), it can be seen that when the metal structure is loaded, the resonant frequency of the corresponding patch antenna decreases as the strain increases. Notably, under the action of stress, the crack monitoring patch will also produce a certain deformation, which in turn leads to a shift in its resonant frequency, thus introducing a small crack monitoring error. Therefore, a certain compensation is needed through the crack strain decoupling algorithm of the microstrip antenna sensor.

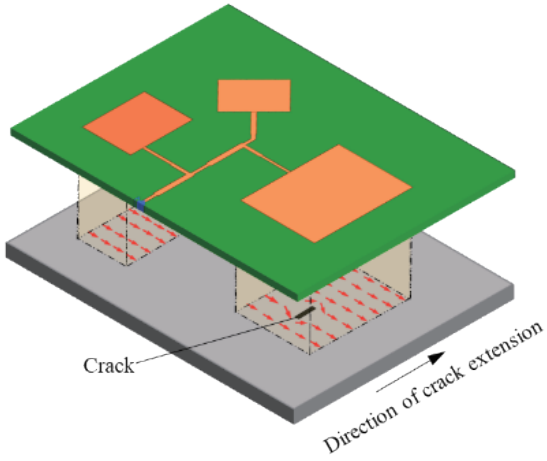

Fig. 3. (Color online) Crack monitoring principle of the antenna sensor array.

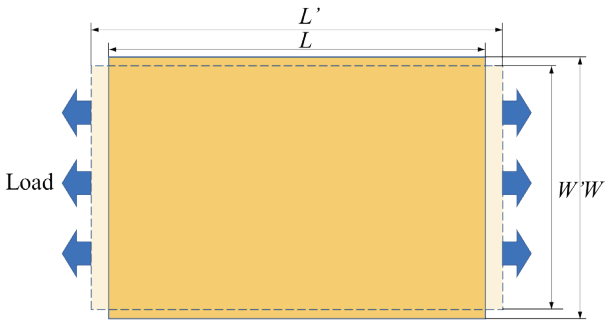

Fig. 4. (Color online) Deformation of the patch of antenna sensor under loading.

3. Antenna Sensor Array Design

3.1 Antenna sensor unit design

The first step in the design of the antenna sensor array is the design of the antenna sensor unit. The strength of the sensor performance of the antenna sensor unit is directly related to that of the sensor array. When calculating the size of each patch, two conditions must be considered: (1) the aspect ratio of the patch must be within a certain range; otherwise, it will cause an abnormal electric field in the resonant cavity of the antenna, thus making the resonant frequency of the antenna abnormal. (2) Because the proposed antenna sensor array uses the frequency division multiplexing method for resonant frequency extraction, the patch size should be determined by considering the interference of the second harmonic. For example, the resonant frequency of the designed crack monitoring patch is 1.5 GHz, and it is known through the theory that it has a second harmonic in the range of 1.5–3 GHz. Additionally, a specific second harmonic is anticipated around 3 GHz. Therefore, when designing the strain detection patch, attention should be taken to avoid interference from the higher harmonics of the crack detection patch and design its resonant frequency outside the two second harmonics.

In this study, the microstrip antenna crack monitoring unit was not designed according to the microstrip antenna dimensioning method described in Sect. 2. The FR4 laminate with a thickness of h = 1 mm and a dielectric constant ε = 4.4 was selected as the substrate material. Considering the effects of the crack monitoring sensitivity and range, the resonant frequency of the crack monitoring unit was selected as 1.55 GHz, and the patch size was designed as L_{c0} = 46 mm and W_{c0} = 60 mm. The microstrip line center side feed was selected as the feed method for the crack monitoring unit, such that only the operating frequency of the sensor in TM_{10} mode is obtained and only the horizontal crack direction is monitored. Considering the microstrip antenna impedance matching problem, we selected the method of changing the feed line width to improve the impedance matching of the sensor. At this time, the feed line acts as a 1/4 wave resistance converter to match the impedance of the radiating patch with an SMA connector of 50 Ω. The width of the feed line is first obtained through the microstrip line characteristic impedance calculation formula and then designed through the parameter scanning function in the high-frequency structure simulator (HFSS). The final feedline width t = 1.2 mm was obtained by optimizing the final resonant frequency to ensure that the return loss is less than −10 dB. The dimensional diagram of the designed crack monitoring unit and the detailed parameters of each part are presented in Fig. 5 and Table 1, respectively.

The simulation model of the microstrip antenna sensor was completed in HFSS by following the steps of solid modeling, material assignment, electromagnetic setup, meshing, parametric scanning, and solving in sequence. The simulated resonant frequency f_r = 1.522 GHz is in basic agreement with the designed resonant frequency of 1.55 GHz; the slight difference is attributed to uneven mesh division.

The design of the strain monitoring cell is similar to that of the crack monitoring cell to avoid repeating the process of calculating the patch size. The specific dimensional design parameters

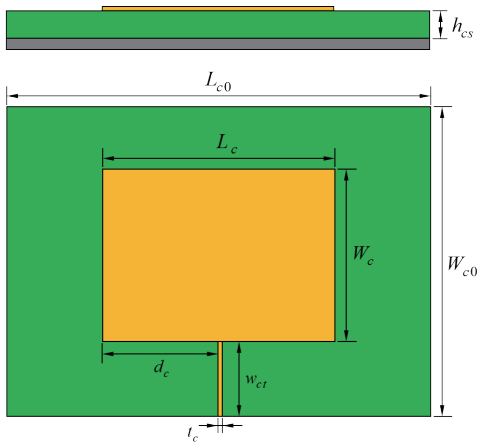

Fig. 5. (Color online) Schematic diagram of the crack monitoring unit.

Table 1
Parameter meaning and numerical table of the crack monitoring unit.

Symbol	Parameter	Numerical value (mm)
h_{cs}	Substrate thickness	1
L_{c0}	Substrate length	120
W_{c0}	Substrate width	86
L	Radiation patch length	60
W	Radiation patch width	46
d_c	Microstrip feeder position	29.4
w_{ct}	Feeder length	20
t_c	Feeder width	1.2

of each patch of the integrated strain and crack monitoring antenna sensor array are shown in Table 2.

3.2 Feeder network design

After the unit design, the antenna units were arranged in a certain order according to the health monitoring requirements. Notably, the feed network of the antenna sensor array had to be designed before the arrangement. In this study, the impedance of the load patch is matched to the feeder network by adjusting the length and width of each feeder, based on the microstrip power divider principle. The specific structure and size of the feed network are presented in Fig. 6 and Table 3, respectively.

3.3 Antenna sensor array fundamental frequency simulation

The HFSS simulation model of the integrated crack and strain monitoring antenna sensor array and the simulation results for the fundamental resonant frequencies are shown in Fig. 7. As can be seen, the return losses at all four resonant frequencies of the design are below −10 dB.

Table 2
Design parameters of each patch in the sensor unit.

Serial number of patch	Size (mm)	Resonant frequency (GHz)
1	Length l_1	—
	Width w_1	1.55
2	Length l_2	1.87
	Width w_2	2.22
3	Length l_3	—
	Width w_3	2.78

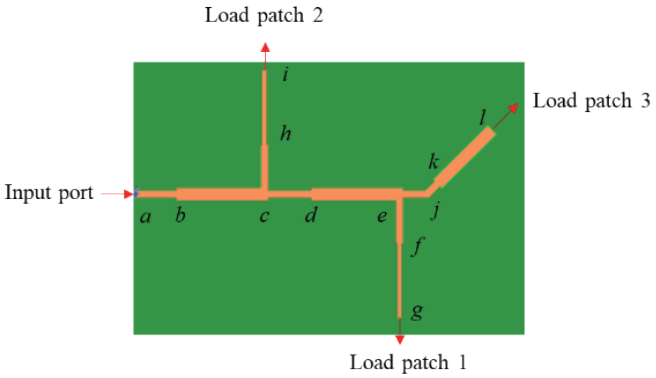

Fig. 6. (Color online) Schematic diagram of feed network design.

Table 3
Design parameters of sensor array feed network.

Feeder section marking	Length (mm)	Width (mm)
ab	10	1.9
bc	21.8	3.2
cd	10	1.9
de	21.8	3.2
ef	10	1.9
fg	17.6	1.2
ch	10	1.9
hi	17.6	1.2
ej	6	1.9
jk	4	1.9
kl	17	2.4

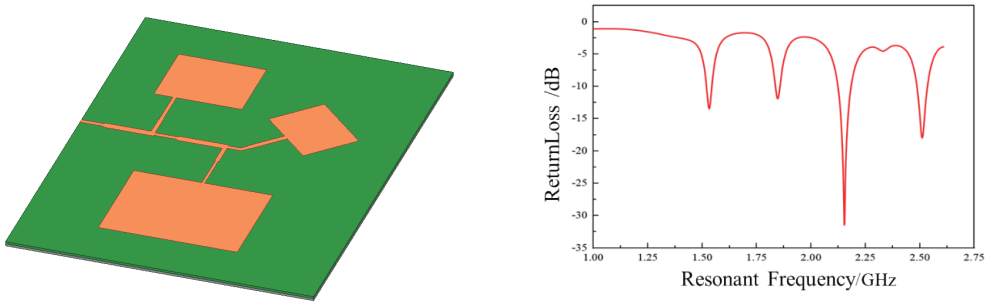

(a) (b)

Fig. 7. (Color online) (a) Simulation model of the array and (b) simulation results of the fundamental resonant frequency.

The four resonant frequencies are 1.5316, 1.8461, 2.1524, and 2.5115 GHz. The resonant frequency at 1.5316 GHz is that of the crack monitoring patch, and the remaining three resonant frequencies are those of the strain monitoring patch. Additionally, a minor sag can be observed at around 2.34 GHz. The analysis reveals that this sag is a subharmonic of the resonant frequency of the crack monitoring patch (1.5 GHz), which does not affect the parameter monitoring of the sensor and can therefore be ignored.

4. Simulation of Antenna Sensor Array Health Monitoring

To verify the crack length monitoring capability of the integrated crack and strain monitoring unit, the HFSS electromagnetic field simulation software was used to simulate the crack extension on the surface of the structure. Similar to the simulation of the crack sensor unit, a penetrating crack of 0.6 mm width was also introduced into the sensor's grounding plate, with the crack position extending from the left edge of Patch 1 to the other end in 5 mm steps over a total extension length of 60 mm, interspersed throughout the patch. The simulation results are shown in Fig. 8.

As shown in Fig. 8, the expansion of the crack only affected the resonant frequency of Patch 1 and had almost no effect on the remaining three resonant frequencies. All four resonant frequencies of the sensor array were unchanged until the crack expanded below Patch 1. Then, the resonant frequency of Patch 1 began to drop, and as the crack length increased, its resonant frequency exhibited a parabolic downward trend, and the sensitivity of crack monitoring was approximately 11.7 MHz/mm. When the crack expanded out of the coverage area of Patch 1, the resonant frequency of Patch 1 still exhibited a downward trend. However, the rate of decline began to slow down and finally stabilized.

A structural strain monitoring simulation with the simulation model shown in Fig. 7(a) was carried out for the proposed integrated monitoring unit to verify its omnidirectional strain monitoring capability. To simplify the analysis of the simulation, the displacements in the

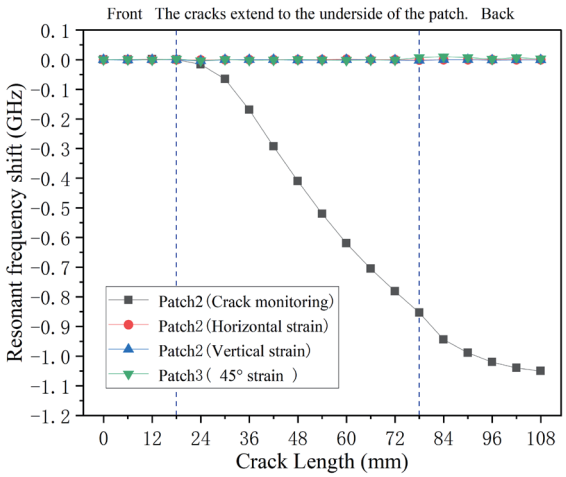

Fig. 8. (Color online) Simulation results of crack propagation of array.

specified directions were applied to the sensor unit separately, which in turn stimulated the strain applied to the sensor under a stress field. Figure 9 shows the relationship between the strain applied to the strain monitoring patch and its resonant frequency.

As shown in Fig. 9, the resonant frequencies of all strain monitoring patches decreased linearly as the applied strain increased. The strain monitoring sensitivities in the transverse, longitudinal, and 45° directions are 1.72, 2.06, and 1.18 kHz/με, respectively.

5. Experimental Design and Data Analysis

5.1 Test platform construction

The test rig consisted of an antenna sensor array, a vector network analyzer (Agilent E5061B; 3 KHz–3 GHz; Agilent Technologies, California, USA), a 50 kN universal tensile tester (THMELX-2), a static strain indicator (XL2101C), a prefabricated crack, a coaxial connector, and strain gauges. The test rig is shown in Fig. 10.

The fabricated antenna sensor array was bonded to the surface of the steel plate using an epoxy resin adhesive and connected to the vector network analyzer through a coaxial connector. We sanded the steel plate at an angle of 45° before bonding to ensure sufficient surface roughness in the sensor area for a reliable adhesive bond. Sanding was performed with cotton gauze dipped in acetone solution with appropriate concentration, and the surface of the steel plate was wiped clean. Then, epoxy resin adhesive was evenly applied to both the steel plate and the surface of the sensor. The sensor was then placed on the corresponding area of the plate. The air bubbles between the sensor and the metal plate were removed by pushing them toward the edges in a single direction. Finally, the pasted steel plate specimen was exposed to the air for about 48 h so that the glue could be fully cured. After the glue was fully cured, we removed the adhesive residue around the sensor and polished the edge of the sensor with sandpaper. The strain gauges were placed on the lower surface of the steel plate in accordance with the resonance pattern of

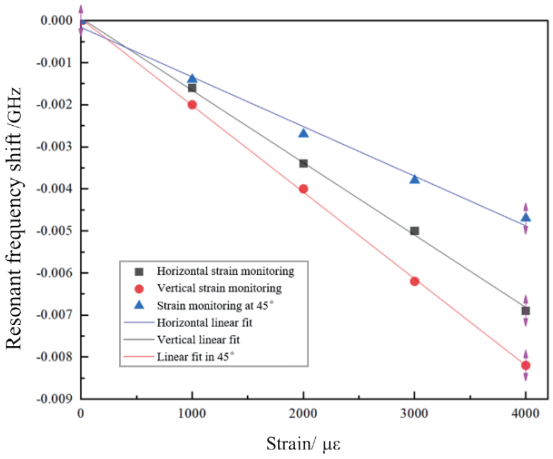

Fig. 9. (Color online) Relationship between strain and resonant frequency of strain monitoring patch.

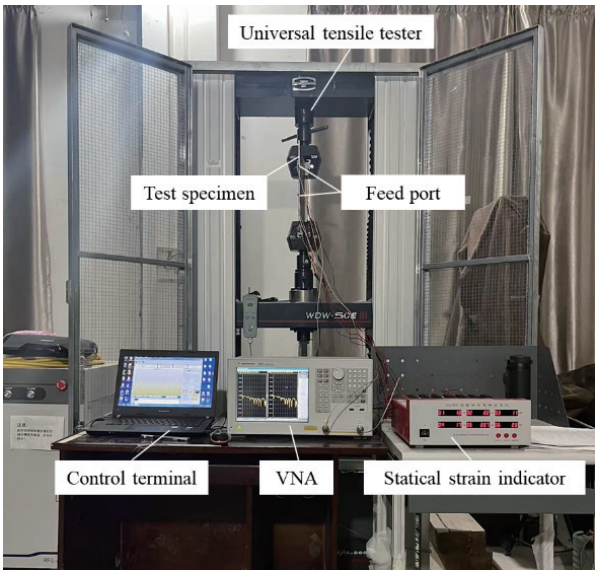

Fig. 10. (Color online) Test platform for crack strain monitoring.

the patch antenna that corresponds to the measurement direction. The strain gauges were connected with the static strain gauge. The sensor array arrangement on both sides of the steel plate specimen is shown in Fig. 11. The samples were preprocessed to simulate crack penetration with different lengths. The cracks were simulated at different lengths between 0 and 90 mm, in 6 mm increments, to represent various stages of crack extension.

5.2 Test procedure

The tests were carried out as follows:

(1) Crack extension monitoring tests were carried out firstly. A steel plate specimen of the antenna sensor array was prepared as described in Sect. 5.1. The response of each crack monitoring array element of the sensor array at different crack lengths was collected using a vector network analyzer. The test was repeated three times in each case, and the final results were averaged.

(2) Strain monitoring tests were subsequently carried out. First, the crack-free specimen was clamped onto the tensile tester. Next, tension was applied to the specimen by setting a certain initial load through the control terminal of the tensile tester. Then, the strain gauge leads were connected to the two-channel terminals of the static strain gauge using a radio frequency cable connected to the SMA connector and the vector network analyzer; the cable was fixed using paper glue to prevent unstable connection caused by the movement of the connection cable during the test. The loading program was deployed to the control terminal of the tensile testing machine, and the load was applied step by step with equal force, with a load range of 0–15 kN and a step size of 3 kN. Each load was held for 180 s, and the vector network analyzer and static strain gauge were used in a steady state for signal acquisition.

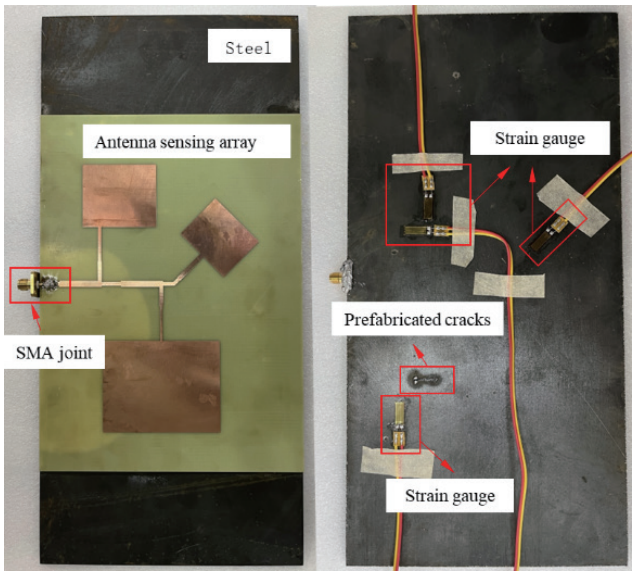

Fig. 11. (Color online) Sample plate of the sensor array.

(3) Simultaneous crack and strain monitoring tests were carried out. As described in step (2), strain monitoring was conducted on specimens with varying crack length. The resonant frequency response of each array element at different crack lengths and strains was obtained using a vector network analyzer. The experimental results were analyzed and are discussed below.

5.3 Analysis of test results

Figure 12 shows the crack extension monitoring test results for the antenna sensor array, which indicate the "crack length–resonant frequency" relationship. As the crack expanded along the length of the crack monitoring unit, the resonant frequency of the crack monitoring unit exhibited a parabolic downward trend. After extending out of the patch coverage area, the resonant frequency continued to decline, but the rate of decline became slower and finally stabilized at approximately 0.55 GHz. However, the resonant frequency of the strain monitoring unit did not change, meaning that the resonant frequency remained stable within 0.02. Therefore, when the crack extended under the crack monitoring unit, the resonant frequency of the strain monitoring unit was not affected. The small fluctuations may be related to manufacturing defects in the specimen and testing equipment. The welding conditions of the SMA joint also have an effect. The SMA connector is not securely connected, which can cause the resonant frequency of the antenna to be shifted.

Figure 13 shows the strain monitoring test results for the antenna sensor array as a "strain magnitude–resonant frequency" plot. The results reveal that the resonant frequency of each patch of the strain monitoring module has an excellent linear relationship with the structural strain, with linearities of 0.992, 0.9942, and 0.9956 for the horizontal, vertical, and 45° strain monitoring processes, and pressure monitoring sensitivities of 1.2721, 2.1063, and 0.7959 kHz/

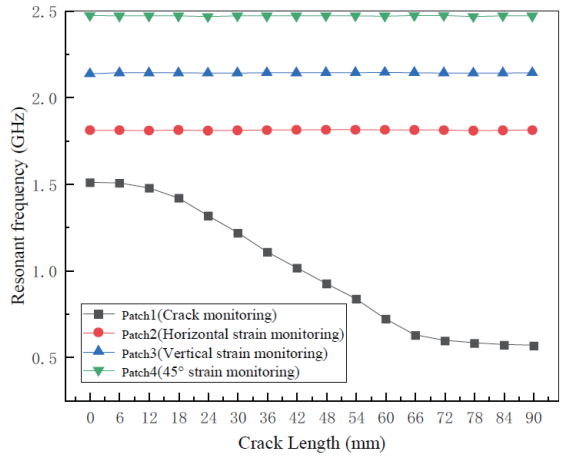

Fig. 12. (Color online) Test results of crack monitoring.

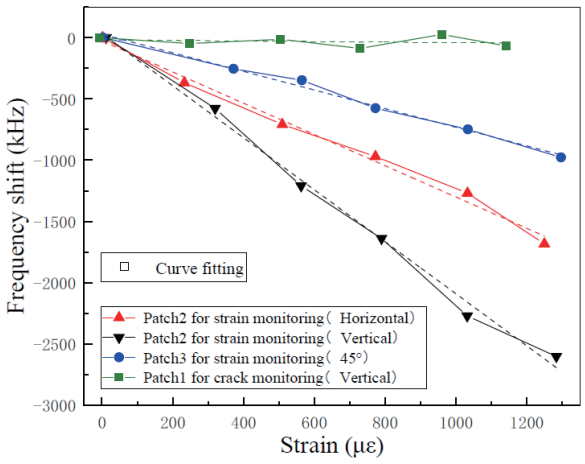

Fig. 13. (Color online) Strain monitoring test results.

με, respectively. Strain transfer loss existed owing to the adhesive layer bonded between the sensor and the jointing plate, resulting in a decrease in strain test sensitivity during the test. However, the overall trend is consistent with the simulation results, and the hot pressing integration can reduce the strain transfer loss caused by the adhesive layer in practical engineering applications. Additionally, it can be seen that the resonant frequency of the crack monitoring patch did not change significantly under loading, and its value fluctuated upward and downward in the vicinity of 1.51 GHz, possibly owing to the large size of the crack monitoring patch design, resulting in reduced strain monitoring sensitivity.

Figure 14 shows the results of the simultaneous strain and crack monitoring experiment using the antenna sensor array. The resonant frequencies of strain monitoring Patches 2 and Patch 3 were converted to stress based on the tension versus the resonant frequency relationship derived from the pressure monitoring tests. Figure 14(a) shows the results of the strain monitoring

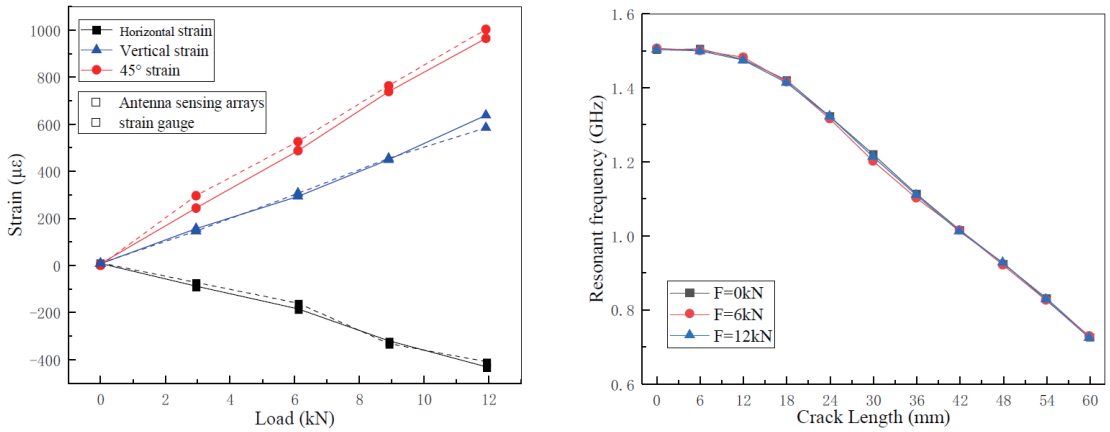

(a) (b)

Fig. 14. (Color online) Test results of simultaneous crack and strain monitoring. (a) Strain monitoring module. (b) Crack monitoring module.

module for the specimen, where the solid line indicates the structural strain monitored by the antenna sensor array, and the dashed line indicates the structural strain monitored by the strain gauges. As can be seen, as the load increased, the horizontal pressure and 45° directional strain applied to the structure decreased, while the vertical strain increased. A certain error exists between the strain values measured by the antenna sensor array and the strain gauge measurements at different load levels, but this error is small (essentially within ±30 με). Therefore, the designed sensor array can meet the requirements of monitoring the strain on the structure.

The test results for steel plate specimens with crack lengths of 0–60 mm at 0, 6, and 12 kN are analyzed. The crack monitoring module results for the specimens are displayed in Fig. 14(b). As can be seen from the graph, the load variation had a minor effect on the crack monitoring results. There are two reasons for this: on one hand, the large size of the crack monitoring patch is designed to have a lower strain test sensitivity; on the other hand, the change in the resonant frequency of the crack monitoring element of the sensor array, which was caused by the structural strain difference, is relatively small for the crack monitoring sensitivity. Therefore, the effect of strain on the resonant frequency of the crack monitoring module can be ignored. The designed sensor array can monitor the structure more effectively, which means that the designed sensor array can monitor the crack generation in the structure more accurately.

6. Conclusions

In this paper, we proposed a method for structural strain and crack length identification based on a microstrip antenna sensor array. The idea of frequency division multiplexing was implemented in the antenna sensor array design to monitor the structural strain and crack length simultaneously. Additionally, theoretical analysis, simulation studies, and experiments for verifying the feasibility of strain monitoring and crack length identification were conducted. The main conclusions drawn from this study are as follows:

1 By applying the idea of frequency division multiplexing to sensor array design, the resonant frequency information of each element of the antenna sensor array can be resolved in the frequency domain only, which solves the problem of reading the resonant frequency of the multiple array elements in the array design in a relatively simple way.
2. The proposed antenna sensor array can identify both the strain and crack length of the structure. The crack monitoring sensitivity of the crack monitoring patch is approximately 13.1 MHz/mm. The strain monitoring sensitivities in the horizontal, vertical, and 45° directions are 1.0783, 1.9466, and 0.7127 kHz/με, respectively.

Acknowledgments

The authors acknowledge the support from the Special Equipment Safety Supervision Inspection Institute of Jiangsu Province and Wuhan University of Technology.

References

1 C. R. Farrar and K. Worden: Phys. Eng. Sci. **365** (2007) 1851. https://doi.org/10.1098/rsta.2006.1928
2 I. Z. Abidin, C. Mandache, G. Y. Tian, and M. Morozov: Ndt & E Int. **42** (2009) 7. https://doi.org/10.1016/j.ndteint.2009.04.001
3 V. Volkovas and J. Dulevicius: Russ. J. Nondestr. Test. **42** (2006) 4. https://doi.org/10.1134/S106183090604005X
4 H. K. Kang, H. J. Bang, C. S. Hong, and C. G. Kim: Meas. Sci. Technol. **13** (2002) 8. https://doi.org/10.1088/0957-0233/13/8/305
5 Y. Kim, Y. Kim, C. Lee, and S. Kwon: IEEE Sens. J. **10** (2010) 8. https://doi.org/10.1109/JSEN.2009.2039565
6 G. Varamini, A. Keshtkar, and M. Naser-Moghadasi: AEU-Int. J. Electron. Commun. **83** (2018) 213. https://doi.org/10.1016/j.aeue.2017.08.057
7 B. Honarbakhsh: AEU-Int. J. Electron. Commun. **75** (2017) 1. https://doi.org/10.1016/j.aeue.2017.02.014
8 I. Mohammad and H. Huang: Smart Mater. Struct. **19** (2010) 5. https://doi.org/10.1088/0964-1726/19/5/055023
9 H. Dong, W. Kang, L. Liu, K. Wei, J. Xiong, and Q. Tan: Meas. Sci. Technol. **30** (2019) 4. https://doi.org/10.1088/1361-6501/ab068a
10 J. Zhang, B. Huang, G. Zhang, and G. Y. Tian: Sensors **18** (2018) 7. https://doi.org/10.3390/s18072130
11 L. Ke, Z. Liu, and H. Yu: Sensors **19** (2018) 1. https://doi.org/10.3390/s19010110
12 U. Tata, H. Huang, R. L. Carter, and J. C. Chiao: Meas. Sci. Technol. **20** (2008) 1. https://doi.org/10.1088/0957-0233/20/1/015201
13 O. Ossa-Molina, J. Duque-Giraldo, and E. Reyes-Vera: IEEE Sens. J. **21** (2021) 20. https://doi.org/10.1109/JSEN.2021.3107136
14 P. Lopato and M. Herbko: Sensors **18** (2018) 1. https://doi.org/10.3390/s18010310
15 X. Xu and H. Huang: Smart Mater. Struct. **21** (2011) 1. https://doi.org/10.1088/0964-1726/21/1/015004
16 X. Yi, C. Cho, J. Cooper, Y. Wang, M. M. Tentzeris, and R. Leon: Smart Mater. Struct. **22** (2013) 8. https://doi.org/10.1088/0964-1726/22/8/085009
17 A. Daliri, A. Galehdar, W. S. T. Rowe, S. John, and C. H. Wang: Sensors **14** (2014) 1. https://doi.org/10.3390/s140100595
18 G. Chakaravarthi, K. P. Logakannan, J. Philip, J. Rengaswamy, V. Ramachandran, and K. Arunachalam: IEEE Sens J. **18** (2018) 12. https://doi.org/10.1109/JSEN.2018.2831903
19 M. Herbko and P. Lopato: Int. J. RF Microwave Comput.-Aided Eng. **29** (2019) 12. https://doi.org/10.1002/mmce.21977
20 Z. Liu, R. Li, J. Yuan, and H. Yu: Meas. Sci. Technol. **31** (2019) 3. https://doi.org/10.1088/1361-6501/ab554c
21 M. Herbko, P. Lopato, G. Psuj, and P. Rajagopal: IEEE Sens. J. **22** (2022) 13. https://doi.org/10.1109/JSEN.2022.3177932
22 L. Chen, L. Liu, L. Kang, Z. Wan, G. Wan, and G. Xie: IEEE Internet Things **10** (2022) 6. https://doi.org/10.1109/JIOT.2022.3221938
23 S. Deshmukh, I. Mohammad, M. Tentzeris, T. Wu, and H. Huang: Smart Mater., Adapt. Struct. Intell. Syst. **2** (2009) 511. https://doi.org/10.1115/SMASIS2009-1326